HTML ABSTRACT

Excited State Fragments Following Molecular Ionization and Dissociation in Strong Fields

John P. Nibarger, Ming Li, Saipriya Menon, George N. Gibson*

Department of Physics, University of Connecticut, Storrs, CT 06269

Abstract.

We have observed for the first time that charge asymmetric dissociation in diatomic molecules leaves one of the fragments in an electronically excited state. Using a new double pulse technique, we determine the state of the post dissociation fragments. For example, we observed the reaction $I_2+(pulse1) \rightarrow (I_2^{2+})^{**} \rightarrow I^{0+}+(I^{2+})^{*}+(pulse2) \rightarrow I^{0+} + I^{3+}$ demonstrating that the I^{2+} fragment must have been in an excited state. More generally, just as asymmetric dissociation implies that the initial molecular ion is in an excited electronic state, the observation of asymmetric channels in the post-dissociation ionization shows that the ionic fragments are themselves electronically excited.

INTRODUCTION

In strong field ionization, final electronic state analysis has largely been neglected. Attention has been primarily focused on ionization rates from a particular initial state rather than the final state of the atom or molecule following ionization. Sequential atomic ionization follows well-understood ionization rates [1] and is independent of any internal structure [2]. This assumes that the initial electronic state of the atom or ion is its ground state implying that little population is left in excited states. A variety of experiments, however, show that molecules can be left in highly excited electronic states with large branching ratios. These experiments include the observation of charge asymmetric dissociation (CAD) in N_2 [3–5], O_2 [3,6], and I_2 [7–9], VUV fluorescence from N_2 [10], and the wavelength dependence of CAD channels [3]. Here, charge asymmetric means a charge difference greater than one. Given the experimental evidence that a molecule can be left in an electronically excited state by strong field ionization, it is important to ask what the relaxation processes for these excited states are and whether they can be controlled? This excitation energy can either be converted into radiation [10], kinetic energy of the dissociation fragments [3–9], or, more significantly, into electronic excitation of the fragments. The latter, although not previously observed, could provide the basis

CP525, *Multiphoton Processes: ICOMP VIII, 8th International Conference,*
edited by L. F. DiMauro, R. R. Freeman, and K. C. Kulander
© 2000 American Institute of Physics 1-56396-946-7/00/$17.00

Downloaded 04 Sep 2009 to 198.11.27.70. Redistribution subject to AIP license or copyright; see http://proceedings.aip.org/proceedings/cpcr.jsp

for efficient and controlled production of excited state ions. With a new double pulse technique called Correlated Ion Spectroscopy (CIS) we can obtain information about the state of the fragments and we have, indeed, observed that CAD can lead to fragments in singly and multiply excited electronic states.

CORRELATED ION SPECTROSCOPY

Single laser pulse measurements using time of flight (TOF) spectroscopy cannot directly reveal whether or not an ion resulting from strong field ionization is in an electronically excited state. Double pulse techniques have been used in strong field physics to show the existence of enhanced ionization at a critical internuclear separation [11], to give experimental evidence for the molecular stabilization hypothesis in strong fields [12], to measure the structure and dynamics of internuclear wave packets [13], and more recently to study the dissociation dynamics of D_2^+ [14]. In the following experiments, we use a new double pulse technique, CIS, to determine the state of the fragments as illustrated by the following example:

$$I_2 + (pulse1) \rightarrow (I_2^{2+})^{**} \rightarrow I^{0+} + (I^{2+})^{*} + (pulse2) \rightarrow I^{0+} + I^{3+} \qquad (1)$$

The first pulse creates an excited molecular state leading to CAD. During the second pulse, I^{0+} acts as a probe of the absolute intensity, in that, the intensity must be below the threshold for ionization. The observation that $(I^{2+})^*$ does ionize shows that it must be in an excited state. Although we cannot directly detect the neutral atom, we can infer that it did not ionize based on the kinematics of the I^{3+} ion, as will be discussed, in detail, below.

CIS also allows us to solve the problem of identifying neutral dissociation channels through correlations. Until now, for diatomic molecular dissociation $I_2^{m+n} \rightarrow I^{m+} + I^{n+}$, the $m+$ and $n+$ fragments could be identified through correlations only if neither was a neutral. Furthermore, correlations are difficult to detect if there is an overlap of the $m+$ or $n+$ peak with other peaks in the TOF spectrum. These limitations can be overcome by varying the delay between the two pulses in the CIS technique. This additional degree of freedom allows us to completely determine a dissociation channel by simply measuring the kinetic energy of one fragment as a function of pulse delay.

In CIS, the first laser (pump) pulse creates some initial molecular charge state, I_2^{m+n}, which then dissociates into the fragments, $I^{m+} + I^{n+}$, hereafter labeled as (m, n). The second (probe) pulse is delayed by a time, τ, and further ionizes the fragments I^{m+} and I^{n+} to I^{m+i} and I^{n+j}, respectively. The energy of the resulting double pulse channel, $(m+i, n+j)$, is measured by using one of the fragments as a function of time delay. The measured energy comes from two sources: the initial dissociation energy of the (m, n) channel and the additional Coulomb energy gained when the second pulse projects the dissociated molecule onto the $(m+i, n+j)$ potential energy curve. The Coulomb energy gained depends on the fragment separation which is in turn controlled by the time delay. Ultimately, this time

Downloaded 04 Sep 2009 to 198.11.27.70. Redistribution subject to AIP license or copyright; see http://proceedings.aip.org/proceedings/cpcr.jsp

dependence can be used to determine the charge state of the undetected fragment. In the limit of large delay, the additional Coulomb energy from the second source is negligible and the energy measured is that of the original dissociation channel, (m,n), called the asymptotic energy, E_{asym}.

In principle, the molecular curves of both the (m,n) and $(m+i,n+j)$ channels are needed to fully predict the resultant kinetic energy of the fragments. We concentrate here on cases where (2,0) is the initial channel, which has a low dissociation energy. Channels starting with fragments that are both ionized will dissociate significantly faster and, thus, will be harder to resolve in time. Assuming a purely Coulombic interaction for the subsequent double pulse channels we can model the energy vs. delay for various charge states. The total energy, E_T as a function of delay is given by:

$$E_T(\tau) = E_{asym} + \frac{(m+i)(n+j)}{r(\tau)}, \tag{2}$$

where

$$r(\tau) = \tau \cdot \ v = \tau \cdot \sqrt{\frac{2E_{asym}}{m}} \tag{3}$$

and $r(\tau)$ is the internuclear separation at the second ionization step.

The energy of the $m+i$ fragment is measured and by changing τ we can determine the charge of the $n+j$ fragment. We have further assumed that the velocity during the time between the two pulses is constant and given by the final asymptotic energy. Ideally, E_{asym} can be measured from the single pulse TOF spectrum for the initial channel (m,n). However, we can also determine a strict lower bound on E_T, without knowing E_{asym}, by analytically minimizing E_T with respect to E_{asym} at each time delay. This process gives the theoretical minimum dissociation energy and will be useful below for identifying certain dissociation channels.

EXPERIMENTAL SETUP

The experiment was performed using a Ti:Sapphire laser system at a 1 kHz repetition rate with 400 μJ per pulse in 30 fs with a center wavelength of 800 nm [15]. The two pulses for the double pulse experiment were created using two beamsplitters. The first beamsplitter was either 50%/50% or 20%/80% and it set the ratio of the pump to probe pulse intensity. The optical path length of one of the pulses was delayed by a retroreflector on a 0.1 μm resolution translation stage. The two beams were then recombined by a 50%/50% beamsplitter. Spacial and temporal overlap of the pump and probe pulses was achieved by observing their interference pattern. Both the pump and probe pulses were identical in polarization and pulse duration, only their intensities were varied.

These pulses are focused by an on-axis parabolic mirror in an ultra high vacuum chamber (base pressure $< 5 \cdot 10^{-10}$ torr). Iodine gas is introduced effusively at

Downloaded 04 Sep 2009 to 198.11.27.70. Redistribution subject to AIP license or copyright; see http://proceedings.aip.org/proceedings/cpcr.jsp

a typical pressure of 10^{-6} torr. A dc field extracts the ions through a 1 mm aperture and they are detected by a microchannel plate at the end of a TOF mass spectrometer. The aperture and the microchannel plate define the axis of the TOF tube and only ions that are aligned with the TOF tube are collected. For each collected ion pair, there is a forward going and backward going fragment, corresponding to initial momentum towards or away from the microchannel plate respectively. Hence, the TOF spectra are made up of pairs of peaks. The peaks in each pair are unequal due to the different collection efficiencies for the forward and backward going fragments. The grid voltages are set so that the pairs of peaks are symmetric with respect to zero kinetic energy arrival time.

Signals from the microchannel plate are amplified, discriminated, and counted by a computer. Ion yields of molecular fragments were obtained by a time convolution of the TOF signal and the gate of a boxcar integrator [16]. The fragment peaks often overlap in the TOF spectra and so the trigger for the boxcar could not be determined absolutely with an oscilloscope. The boxcar gate was scanned through the original TOF signal creating a correlation of the two. From this scan we were able to accurately set the trigger. The absolute intensity is calibrated by fitting the Ar^+ ion yield (IY) to the Ammosov, Delone, Krainov (ADK) model [1,17].

EXPERIMENTAL RESULTS

Typical TOF spectra for I^{3+} are shown in Fig. 1. We have observed a new pair of low energy peaks between the (3,1) pair and the zero kinetic energy peak when we use the double-pulse beam. The pairs of single pulse peaks are unaffected by the presence of the second pulse as the intensities required to ionize these atomic charge states is too high. As expected, the energy of the new peaks depends on pulse delay. Figure 2 shows the energy as a function of time delay of the I^{3+} TOF spectra for two different intensity ratios, 1:1 and 1:4, of the first to second pulse. Although one usually uses a weak probe, in this experiment the probe acts on atomic fragments while the pump interacts with a molecule. Since atoms are more difficult to ionize than molecules, the probe pulse needs to be as strong or stronger than the pump pulse. For the 1:4 ratio, the data was fit to the energy vs. delay model (Eq. 2) for the (3,1) channel with a fixed asymptotic energy of 0.8 eV. By measuring its asymptotic energy, the initial state of the (3,1) channel was found to be the (2,0) channel or, less likely, the (1,0) channel:

$$I^{0+} + (I^{2+})^* + (pulse2) \rightarrow I^{1+} + I^{3+} \tag{4}$$

For the 1:1 ratio, however, it was not possible to fit the data to the energy vs. delay model for the (3,1) channel for any fixed asymptotic energy. The theoretical minimum dissociation energy curve (described above) was also calculated for the (3,1) channel. The data were below this curve showing that it is kinematically impossible for the dissociation to have originated from a (3,1) channel and therefore must have come from the (3,0) channel. The initial state of the (3,0) channel was

Downloaded 04 Sep 2009 to 198.11.27.70. Redistribution subject to AIP license or copyright; see http://proceedings.aip.org/proceedings/cpcr.jsp

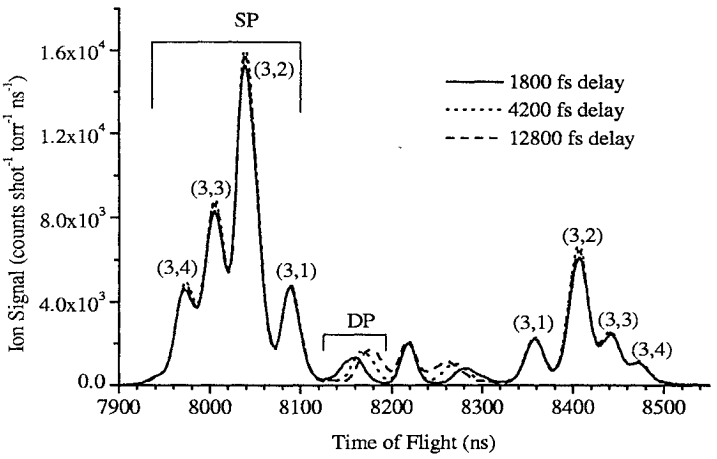

FIGURE 1. Single pulse and double pulse TOF spectrum of I^{3+} for 1800, 4200, and 12800 fs delays with 1:4 intensity ratio between the two pulses where the peak intensity of the pump pulse is $2 \cdot 10^{14}$ Watts/cm^2.

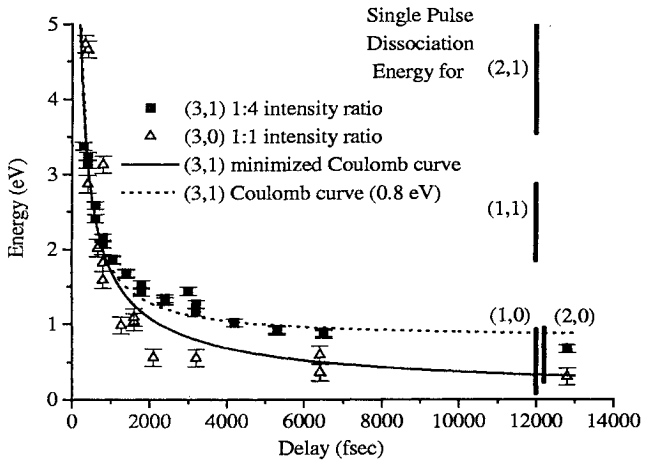

FIGURE 2. I^{3+} energy vs. delay for 1:1 and 1:4 intensity ratios where the peak intensity of the pump pulse is $2 \cdot 10^{14}$ Watts/cm^2. Also included are the theoretical minimum dissociation energy curve for the (3,1) channel and a fit to the energy vs. delay model for 0.8 eV.

Downloaded 04 Sep 2009 to 198.11.27.70. Redistribution subject to AIP license or copyright; see http://proceedings.aip.org/proceedings/cpcr.jsp

again found to have come from the (2,0) channel by measuring the asymptotic energy, Eq. (1). In both these cases, the ionization of the I^{2+} fragment is unexpected as there is not sufficient intensity to ionize the I^{0+} (1:1) or I^{1+} (1:4) fragment. Thus, the I^{2+} must be in an excited state.

Figure 3 shows single pulse ion yield (IY) curves for the (1,1), (2,0), and (2,1) channels and the predicted I^{1+}, I^{2+}, and I^{3+} ion yields from the ADK tunneling ionization model. The IY curves confirm the previous analysis of the difference in final states produced by the 1:1 and 1:4 intensity ratios. For the purpose of this discussion, we will use the threshold values indicated by the IY curves. For the 1:1 ratio, the first pulse creates an initial (2,0) dissociation channel. The second pulse acts on these well separated atoms where the ionization rates are assumed to be described by the ADK tunneling ionization model. According to the ion yields, the second pulse is near the threshold to ionize neutral atomic iodine. Thus, it is likely that a significant fraction of neutral iodine will survive. Clearly, the second pulse is far below the threshold for ionization of I^{2+} in its ground state and since I^{2+} is observed to ionize, I^{2+} must be in an excited state. For the 1:4 ratio, the first pulse again creates the (2,0) dissociation channel. The second pulse is now four times more intense and hence exceeds the threshold for ionization of I^{0+} and I^{1+}. This opens up the new channels (2,0) $\rightarrow$ (3,1) and (3,2). (2,0) $\rightarrow$ (3,3) is still not accessible and (2,0) $\rightarrow$ (3,0) can no longer survive at this intensity.

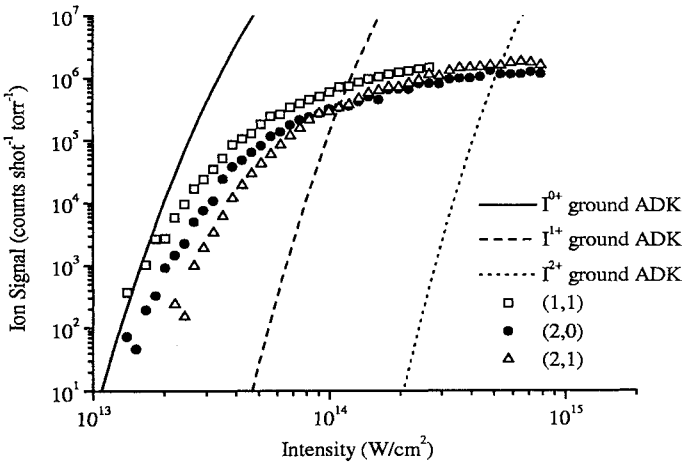

FIGURE 3. Ion yields of molecular fragments (1,1), (2,0), (2,1) and theoretical ion yields for I^{1+}, I^{2+}, and I^{3+} based on the ADK tunneling model.

Although we won't consider them here, other channels have been observed [18] at the 1:4 intensity ratio such as the $(I^{2+})^{**} + I^{0+} \rightarrow I^{4+} + I^{1+}$ and $I^{4+} + I^{2+}$. The remarkable fact here is that while the I^{2+} ground state cannot be ionized, $(I^{2+})^{**}$

Downloaded 04 Sep 2009 to 198.11.27.70. Redistribution subject to AIP license or copyright; see http://proceedings.aip.org/proceedings/cpcr.jsp

can doubly ionize to I^{4+}. Thus the $(I^{2+})^{**}$ fragment must be in a doubly excited state.

Before we make a detailed comparison with tunneling models, we need to rule out amplified stimulated emission (ASE) as a possible cause of these new low energy peaks. ASE from our multi-pass amplifier has a pulse duration of 100 ns and can lead to low energy photo-dissociation of I_2. Therefore, it must be addressed as a possible cause for the secondary low energy peaks in the TOF spectrum. ASE can be varied temporally by injecting the short pulse at different times into the amplifier. If we inject early/late a minimal/typical amount a ASE is obtained. Three pulse interactions are possible if we take into account the 100 ns ASE pulse with the two 30 fs pulses. If the low energy peaks were ASE dependent, then as the amount of ASE is varied the energy of these peaks would change both temporally and in amplitude. We measured the TOF of I^{3+} using a constant amount of short pulse energy while varying the ASE energy [7] shown in Fig. 4. We know that the intensity of the short pulse is constant because the single pulse peaks only depend on the short pulse intensity. Any process that depends on ASE would change in the same way as the zero kinetic energy peak (which is known to result from ASE [7]). Going from a typical to a minimum amount of ASE the zero kinetic energy peak is greatly reduced, whereas the single pulse and double pulse peaks due to the short pulses are not affected. This demonstrates that the double pulse peaks do not depend on ASE.

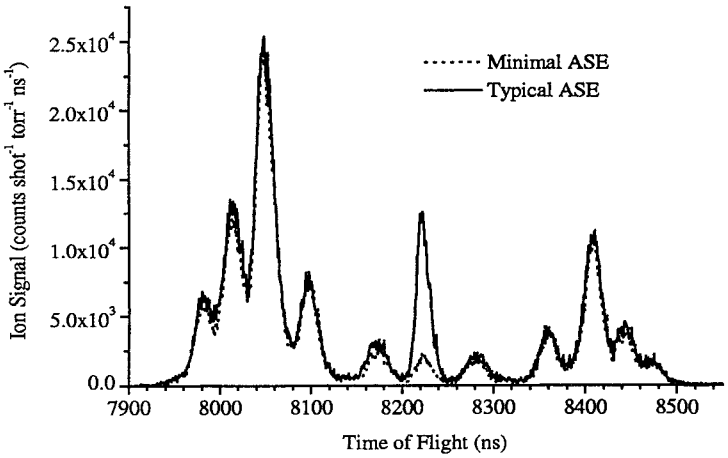

FIGURE 4. TOF spectrum of I^{3+} for two levels of ASE with a peak intensity of the pump pulse is $2 \cdot 10^{14}$ Watts/cm^2.

Downloaded 04 Sep 2009 to 198.11.27.70. Redistribution subject to AIP license or copyright; see http://proceedings.aip.org/proceedings/cpcr.jsp

COMPARISON WITH IONIZATION MODELS

The lack of ionization of the I^{0+} places a firm upper bound on the intensity of the probe pulse. This, in turn, can set a lower bound on the level of excitation of the $(I^{2+})^*$ which does ionize. However, to find this lower bound we need to have some knowledge of the ionization rate of the excited state of an ion. Barrier suppression ionization (BSI) [19] and ADK can certainly be applied to excited states, but it is not clear that they are valid. ADK appears not to work for highly excited states in microwave ionization [20]. However, in 1-dimension, we can set some limits by using an exact tunneling model [21] to compare $I^0 \rightarrow I^{1+}$ ground state ionization with $(I^{2+})^* \rightarrow I^{3+}$ excited state ionization.

The tunneling model can be implemented to calculate rates for each excited state as well as the stark shifted energy of each state. Schrödinger's equation can be solved for the field-free ionization potentials that are used by the ADK model. In order to compare the 3-dimensional ADK model to the 1-dimensional tunneling model, a correction involving averaging over the solid angle has to be made. In practice, this is done by shifting the intensity axis of the ADK model for the ground state to match up with the tunneling calculations for the ground state. Ionization yields for ground state I^{0+} and the first 3 states of I^{2+} are shown in Fig. 5. Also included in Fig. 5 is the BSI model as a reference for complete saturation of the specific channel. Note the excellent agreement between all of the models for excited states.

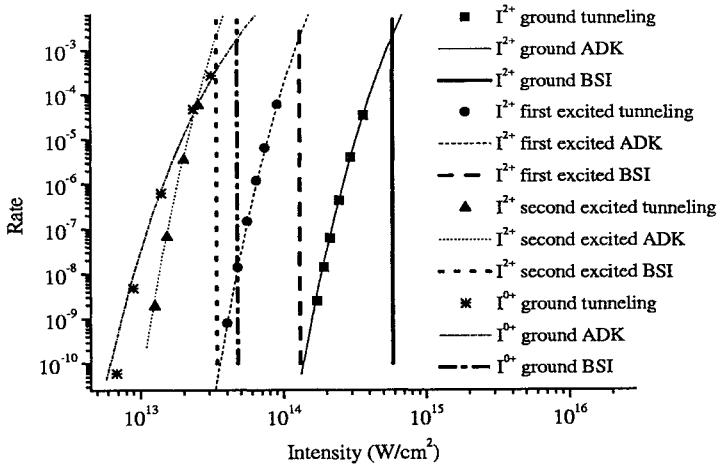

FIGURE 5. Ion yields for comparison of BSI, ADK and tunneling models.

By comparing ADK curves for the ground state ionization of I^{0+} to the excited state curves of $(I^{2+})^*$, we see that the second excited state of the $(I^{2+})^*$ is the

Downloaded 04 Sep 2009 to 198.11.27.70. Redistribution subject to AIP license or copyright; see http://proceedings.aip.org/proceedings/cpcr.jsp

TABLE 1. Ionization potentials and $(I^{2+})^*$ excitation energies for various I^{0+} ionization probabilities.

$\text{Probability}_{0\rightarrow 1}$	$\text{Probability}_{2\rightarrow 3}$	$(I^{2+})^*$ IP	$(I^{2+})^*$ excitation energy
10	90	15.4 eV	17.8 eV
50	50	16.8 eV	16.4 eV
90	10	18.0 eV	15.2 eV

lowest excited state that is still easier to ionize than the I^{0+} at the same intensity. Of course this is only a lower bound, more highly excited states could be populated and still be consistent with the observations.

To place stricter limits on the excitation energy, we would need to know the exact ionization probability for I^{0+} and I^{2+}. Since we cannot measure these directly we can vary the ionization potential of I^{2+} that is put into the ADK model to give specific probabilities that match up to probabilities of the I^{0+} ground state ionization. For example, at 10% probability of ionization of for the I^{0+}, an ADK curve can be created to have a 90% probability of ionizing $(I^{2+})^*$ at that same intensity. The excitation energy of the $(I^{2+})^*$ is then just the difference between the excited state ionization potential and the ground state ionization potential. The ground state ionization potential for I^{2+} is 33.2 eV. Ionization potentials for various probabilities and corresponding $(I^{2+})^*$ excitation energies are shown in Table 1. The excitation energies observed in Table 1 are well above the ground state configuration $5s^25p^3$, and may correspond to an excitation of the $5s5p^4$, $5s^25p^26s$, or $5s^25p^25d$ electronic configurations based on comparison with the Te^{1+} and Xe^{3+} isoelectronic species [22].

By comparison, the field-free ground state excitation of asymmetric channels over symmetric channels is 8.7 eV for (2,0) over (1,1) and 14.1 eV for (3,1) over (2,2) [7]. In other words, the minimum energy of the initial molecular excitation in an asymmetric state is of the same order as the electronic excitation energy of the dissociated atom from that asymmetric state (see Table 1). Therefore, it appears that the excitation energy of the asymmetric state of the molecule has been transferred to electronic excitation in the dissociated fragments.

We made a more extensive comparison in I^{1+} up to the 5th excited state. Figure 6 shows the ionization rate for I^{+1} for the ground state up to the 5th excited state calculated using the 1-dimensional tunneling model and the ADK model. Both the models seem to match up well for the lower excited states. However, starting with the 3rd excited state, the ADK model begins to overestimate the ionization rate and becomes progressively larger for each higher excited state. This deviation can be qualitatively understood by the following explaination. In the presence of the laser field, the ionization potential becomes larger due to the stark shift. Since the field-free ionization potentials are used in the ADK model, the ADK model will predict ionization at a higher rate than the 1-dimensional model.

Downloaded 04 Sep 2009 to 198.11.27.70. Redistribution subject to AIP license or copyright; see http://proceedings.aip.org/proceedings/cpcr.jsp

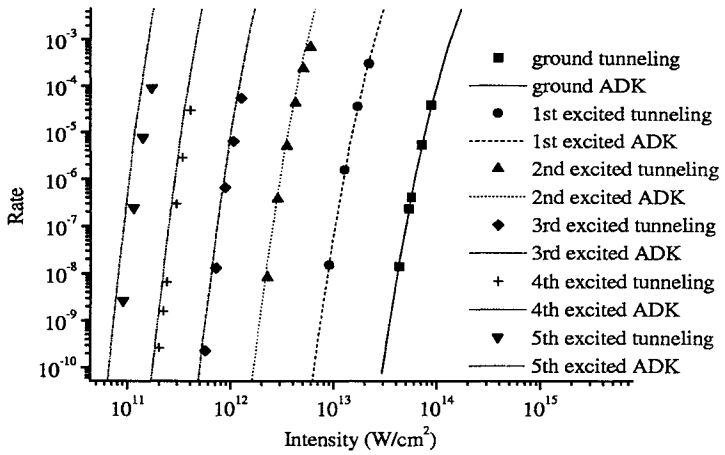

FIGURE 6. Excited state ion yields of I^{1+} for comparison of tunneling and ADK models.

CONCLUSION

Using a new double pulse technique called Correlated Ion Spectroscopy, we demonstrate that charge asymmetric dissociation leaves the fragments in singly or multiply excited electronic states. The observation of excited state fragments from dissociation imply an energy transfer from molecular excitation to atomic excitation. With a high branching ratio of 15-30% for asymmetric states [7], the possibility exists for the direct efficient production of highly excited electronic states from a non-resonant laser pulse. Such production of excited states can potentially be used for VUV and soft x-ray lasers [23].

We would like to acknowledge support from the NSF under Grant No. PHY-9502935. G.N.G. was also supported through funding as a Cottrell Scholar of Research Corporation.

*Electronic address: gibson@phys.uconn.edu

REFERENCES

1. M.V. Ammosov, N.B. Delone, and V.P. Krainov, Sov. Phys. JETP **64**, 1191 (1986).
2. T.D. Walsh, F.A. Ilkov, J.E. Decker, and S.L. Chin, J. Phys. B. **27**, 3767 (1994).
3. C. Guo, M. Li, and G.N. Gibson, Phys. Rev. Lett. **82**, 2492 (1999).
4. K. Boyer, T.S. Luk, J.C. Solem, and C.K. Rhodes, Phys. Rev. A **39**, 1186 (1989).
5. C. Cornaggia, J. Lavancier, D. Normand, J. Morellec, and H.X. Liu, Phys. Rev. A. **42**, 5464 (1990).

Downloaded 04 Sep 2009 to 198.11.27.70. Redistribution subject to AIP license or copyright; see http://proceedings.aip.org/proceedings/cpcr.jsp

6. D. Normand, C. Cornaggia, J. Lavancier, J. Morellec, and H.X. Liu, Phys. Rev. A. **44**, 475 (1991).
7. G.N. Gibson, M. Li, C. Guo, and J.P. Nibarger, Phys. Rev. A. **58**, 4723 (1998).
8. D.T. Strickland, Y. Beaudoin, P. Dietrich, and P. B. Corkum, Phys. Rev. Lett. **68**, 2755 (1992).
9. J.H. Posthumus, A.J. Giles, M.R. Thompson, and K. Codling, J. Phys. B **29**, 5811 (1996): J.H. Thompson, K. Codling, L.J. Frasinski, and M.R. Thompson, Laser Phys. **7**, 813 (1997).
10. G. Gibson, T.S. Luk, A. McPherson, K. Boyer, and C.K. Rhodes, Phys. Rev. A **40**, 2378 (1989).
11. E. Constant, H. Stapelfeldt, and P.B. Corkum, Phys. Rev. Lett. **76**, 4140 (1996).
12. M. Schmidt, P. D'Oliveira, P. Meynadier, D. Normand, and C. Cornaggia, J. Nonlin. Opt. Phys. Materials. **4**, 817 (1995).
13. H. Stapelfeldt, E. Constant, H. Sakai, and P. Corkum, Phys. Rev. A **58**, 426 (1998).
14. C. Trump, H. Rottke, and W. Sandner, Phys. Rev. A **59**, 2858 (1999).
15. M. Li and G.N. Gibson, J. Opt. Soc. Am. B **15**, 2404 (1998).
16. C. Guo, M. Li, J.P. Nibarger, and G.N. Gibson, submitted to Phys. Rev. A.
17. C. Guo, M. Li, J.P. Nibarger, and G.N. Gibson, Phys. Rev. A **58**, 4271 (1998).
18. J.P. Nibarger, M. Li, S. Menon, and G.N. Gibson, Phys. Rev. Lett. **83**, 4975 (1999).
19. S. Augst, D.D. Meyerhofer, D. Strickland, and S.L. Chin, J. Opt. Soc. Am. B, **8**, 858 (1991).
20. B.E. Sauer, S. Yoakum, L. Moorman, and P.M. Koch, Phys. Rev. Lett. **68**, 468 (1992).
21. G.N. Gibson, G. Dunne, and K.J. Berquist, Phys. Rev. Lett. **81**, 2663 (1998).
22. C.E. Moore, "Atomic Energy Levels, Volume 3," (U.S. Government Printing Office, Washington, D.C., 1971).
23. M.Y. Ivanov and P.B. Corkum, Phys. Rev. A, **48**, 580 (1993).

Downloaded 04 Sep 2009 to 198.11.27.70. Redistribution subject to AIP license or copyright; see http://proceedings.aip.org/proceedings/cpcr.jsp